Synthesis of rutherfordium isotopes in the $^{238}U(^{26}Mg, xn)^{264-x}Rf$ reaction and study of their decay properties

J. M. Gates,[1,2] M. A. Garcia,[1,2] K. E. Gregorich,[1] Ch. E. Düllmann,[1,2,3] I. Dragojević,[1,2] J. Dvorak,[4,*] R. Eichler,[5,6] C. M. Folden III,[1,2,†] W. Loveland,[7] S. L. Nelson,[1,2] G. K. Pang,[2,†] L. Stavsetra,[1] R. Sudowe,[1,‡] A. Türler,[4] and H. Nitsche[1,2]

[1] *Nuclear Science Division, Lawrence Berkeley National Laboratory, Berkeley, CA 94720, USA*

[2] *Department of Chemistry, University of California, Berkeley, Berkeley, CA 94720-1460, USA*

[3] *Bereich Schwere Elemente, Gesellschaft für Schwerionenforschung mbH, 64291 Darmstadt, Germany*

[4] *Institut für Radiochemie, Technische Universität München, 85748 Garching, Germany*

[5] *Labor für Radio- und Umweltchemie, Paul Scherrer Institut, CH-5232 Villigen PSI, Switzerland*

[6] *Departement für Chemie und Biochemie, Universität Bern, CH-3012 Bern, Switzerland*

[7] *Department of Chemistry, Oregon State University, Corvallis, OR 97331, USA*

(Received

Isotopes of rutherfordium ($^{258-261}Rf$) were produced in irradiations of ^{238}U targets with ^{26}Mg beams. Excitation functions were measured for the 4*n*, 5*n* and 6*n* exit channels. Production of ^{261}Rf in the 3*n* exit channel with a cross section of 28^{+92}_{-26} pb was observed. Alpha-decay of ^{258}Rf was observed for the first time with an α-particle energy of 9.05±0.03 MeV and an α/total-decay branching ratio of 0.31±0.11. In ^{259}Rf, the electron capture/total-decay branching ratio was measured to be 0.15±0.04. The measured half-lives for ^{258}Rf, ^{259}Rf and ^{260}Rf were $14.7^{+1.2}_{-1.0}$ ms, $2.5^{+0.4}_{-0.3}$ s and $22.2^{+3.0}_{-2.4}$ ms, respectively, in agreement with literature data. The systematics of the α-decay Q-values

and of the partial spontaneous fission half-lives were evaluated for even-even nuclides in the region of the N = 152, Z = 100 deformed shell. The influence of the N = 152 shell on the α-decay Q-values for rutherfordium was observed to be similar to that of the lighter elements ($96 \leq Z \leq 102$). However, the N = 152 shell does not stabilize the rutherfordium isotopes against spontaneous fission, as it does in the lighter elements ($96 \leq Z \leq 102$).

PACS numbers: 25.60.Pj, 25.85.Ca, 23.60.+e, 27.90.+b

I. INTRODUCTION

Relatively long-lived transactinide elements (i.e., elements with atomic number $Z \geq 104$) up to Z = 108 have been produced in nuclear reactions between low Z projectiles (C to Al) and actinide targets. Cross sections have been observed to decrease steeply with increasing Z and reach the level of a few picobarns for element 108 [1]. Recently, production cross sections of several picobarns have been reported [2-4] for comparatively neutron-rich nuclides of 112 through 118 produced via hot fusion reactions with ^{48}Ca and actinide targets. Some of those heavy nuclides are reported to have lifetimes on the order of seconds or longer. The relatively high cross sections in these hot fusion reactions are not fully understood and this has renewed interest in systematic studies of heavy-ion reactions with actinide targets.

Here we report on the measurement of the excitation functions for the 4*n*, 5*n*, and 6*n* exit channels of the ^{238}U(^{26}Mg, x*n*)$^{264-x}$Rf reaction (where x = 4, 5 or 6 and represents the number of neutrons evaporated from the compound nucleus). An additional

experiment was dedicated to the investigation of the 3*n* exit channel to access the comparatively neutron-rich isotope, ^{261}Rf. Combined with data from the ^{238}U(^{30}Si, x*n*)$^{268-x}$Sg reaction [5] and other reactions with ^{238}U targets [6], these results further our understanding of hot fusion reactions. The decay properties of $^{258-260}$Rf have also been studied in depth and the results are reported here. Few previous experiments on the direct production of $^{258-260}$Rf have been sensitive to both α-decay and spontaneous fission (SF). This led to debate over the decay properties of ^{259}Rf [7] and limited the information on the decay properties of ^{258}Rf.

II. EXPERIMENTAL TECHNIQUE

Beams of magnesium ($^{26}Mg^{6+}$) were produced from enriched metallic Mg in the Advanced Electron Cyclotron Resonance (AECR) ion source and then accelerated by the 88-Inch Cyclotron at Lawrence Berkeley National Laboratory (LBNL) to energies of 4.9 - 6.0 MeV/nucleon. The beam passed through a 45-μg/cm^2 thick carbon (C) window at the entrance of the Berkeley Gas-filled Separator (BGS) [8-10] that serves to separate the vacuum of the beam line from the 66-Pa helium (He) gas inside the BGS. Approximately one centimeter downstream of the entrance window was a rotating (~10 Hz) target wheel consisting of nine arc-shaped uranium(IV) tetrafluoride (UF_4, ~470 μg/cm^2) targets. These targets were prepared by evaporation of UF_4 onto 580 μg/cm^2 aluminum (Al) foils. The energy thickness of the UF_4 layer on each target segment was approximately 2.0 MeV.

Typical beam intensities ranged from 0.5 to 1.0 particle-μA. Energy losses in C, Al, and UF_4 were calculated with SRIM2006.02 [11]. The product of target thickness

and beam intensity was monitored on-line by the detection of Rutherford-scattered particles in two PIN diode detectors located at ±27° from the beam axis. Analysis of the pulse heights of the Rutherford-scattered projectiles from the various ^{26}Mg beam energies gives relative energies to within 0.1%. The resulting center-of-target beam energies were 121.8, 128.1, 133.0, 138.5, 144.5 and 151.4 MeV in the laboratory frame. Systematic uncertainty in the energies from the 88-Inch Cyclotron is estimated to be ~1%. Compound nucleus excitation energies were calculated using the relative beam energies with the experimental mass defects for ^{26}Mg and ^{238}U [12] and the Thomas-Fermi mass defects for the compound nucleus [13]. The resulting ranges of compound nucleus excitation energies within the targets were 35.3±0.9, 41.0±0.9, 45.4±0.9, 50.4±1.3, 55.8±0.9 and 62.0±0.9 MeV.

Rutherfordium compound nucleus evaporation residues (EVRs) are formed with the momentum of the projectile and recoil from the target. These EVRs were separated from the beam and other unwanted reaction products in the BGS based upon their differing magnetic rigidities in He gas. Magnetic rigidities of the rutherfordium EVRs were estimated as previously described [9]. The efficiency for collecting rutherfordium EVRs at the BGS focal plane was modeled using a Monte Carlo simulation of the EVR trajectories in the BGS, as described earlier [9, 10], and resulted in efficiencies (ε_{BGS}) of 15-22%, depending on the beam energy (see Table II). Details of the Si-strip detector array and data acquisition system have been reported earlier [9, 14]. The rutherfordium EVRs have a short range and low implantation energy in the focal plane detector due to their low kinetic energy. Thus, a multi-wire proportional counter could not be used and no information was available to help differentiate between implantation events and decay

events of similar energy within the focal plane detector.

The search for EVR-α and EVR-α-α correlations was expected to be hindered by random correlations of events unrelated to the decay of the desired nuclides. This problem was circumvented by using a pulsed beam that had a 50% duty factor with a period of 600 ms. The pulsed beam was used during the 128.1 MeV irradiation and portions of the 121.8, 133.0 and 138.5 MeV irradiations, where significant production of rutherfordium isotopes with a substantial α-decay branch was expected. Searching for α-particles between beam pulses led to a significant background reduction and allowed the identification of the α-emitting nuclides (see Section III.E). To further reduce random correlations during both pulsed and DC irradiations, α-decays were defined as events anticoincident with the upstream detectors, (i.e., the full energy of the α-decay was required to be in the focal plane detector and not split between the focal plane and upstream detectors). A fast shutoff mode was employed to search for ^{261}Rf during the pulsed portion of the 121.8 MeV irradiation. During this mode, the beam was shut off for 100 s after detection of an EVR [3.5 < E(MeV) < 10.0, during the beam pulse] followed by the observation of an α-particle [8.0 < E(MeV) < 9.0, in-between beam pulses] in the same strip and within 300 s and ±3.5 mm of the EVR. This allowed for the detection of the 25-s ^{257}No daughter [15] in nearly background free conditions. Measurements at all other beam energies and the remaining portions of the 121.8, 133.8 and 138.5 MeV irradiations were carried out with a DC beam.

^{259}Rf was identified during pulsed portions of the irradiations using EVR-α correlations that consisted of an EVR [5.0 < E(MeV) < 12.0, during the beam pulse] followed by an α-particle [8.7 < E(MeV) < 9.2, in-between beam pulses] within 10 s and

a vertical position of ±2.0 mm in same strip. During DC beam irradiations, ^{259}Rf was identified by EVR-α-α correlations consisting of an EVR [5.0 < E(MeV) < 12.0] followed by a ^{259}Rf α-particle [8.7 < E(MeV) < 9.2] within 10 s and a ^{255}No α-particle [7.4 < E(MeV) < 8.4] within 560 s. Both α-particles were required to be in the same strip as the EVR and within a vertical position of ±2.0 mm of the EVR. An electron capture (EC) branch in ^{259}Rf was searched for in the pulsed irradiations by the detection of an EVR [5.0 < E(MeV) < 12.0, during the beam pulse] followed by a ^{259}Lr α-particle [8.4 < E(MeV) < 8.5, in-between beam pulses] in the same strip within 15 s and a vertical position of ±2.0 mm. EVR-SF correlations for ^{259}Rf/^{259}Lr were observed during the pulsed and DC modes by detection of an EVR [5.0 < E(MeV) < 12.0] followed by a position (±2.0 mm in the same strip) correlated SF [E(MeV) > 100 MeV] within 15 s.

^{258,260}Rf were identified by the detection of an EVR [3.0 < E(MeV) < 12.0] followed by a time (<150 ms) and position (±2.0 mm) correlated SF [E(MeV) > 100 MeV] event in the same strip. An α-branch in ^{258}Rf was searched for by the detection of an EVR implantation followed by the detection of a ^{258}Rf α-particle [8.0 < E(MeV) < 9.5] within 150 ms followed by a ^{254}No α-particle [7.8 < E(MeV) < 8.3] within 220 s. An α-branch in ^{260}Rf was searched for by the detection of an EVR implantation followed by the detection of a ^{260}Rf α-particle [8.0 < E(MeV) < 9.5] within 150 ms followed by a ^{256}No α-particle [8.2 < E(MeV) < 8.6] within 15 s. Alpha particles in each decay series were required to be in the same strip and within a vertical position of ±2.0 mm of the EVR.

III. RESULTS

A. ^{258}Rf

Seventy-eight EVR-SF correlations were observed at the three highest ^{26}Mg beam energies. These events were assigned to the 6*n* exit channel, ^{258}Rf, as i) both neighboring even-odd nuclides have longer half-lives and decay mainly by emission of α-particles and ii) the reaction energy was at least 29.4 MeV above the threshold for the 4*n* exit channel product. At these excitation energies, the evaporation of more than four neutrons is expected. The total kinetic energy (TKE) of the ^{258}Rf SF was ~8 MeV above the TKE measured for ^{252}No under the same detection setup, similar to what was observed by Wild *et al*. [16].

At the two highest ^{26}Mg beam energies, four observed EVR-α-α correlations were assigned to an α-decay branch in ^{258}Rf (see Table I). Assignment of these events to ^{258}Rf instead of the neighboring ^{259}Rf was based on the observed short lifetimes of the mother followed by a second α-decay consistent with the known properties of the daughter, ^{254}No. Three of the mother events had an average α-particle energy of 9.05±0.03 MeV, likely corresponding to decay from the ground state of ^{258}Rf to the ground state of ^{254}No. The second observed event had an energy 90 keV lower. This event is tentatively assigned to an α-decay from the ground state of ^{258}Rf to an excited state of the daughter in ^{254}No. Based upon the 3 events observed with an average α-particle energy of 9.05±0.03 MeV, the Q-value for the α-decay of ^{258}Rf is 9.23±0.03 MeV after including a 43 keV correction for electron screening [17, 18]. Using the experimental mass defects for ^{254}No and ^{4}He [12], the mass defect of ^{258}Rf was measured to be 96.38±0.05 MeV, in good agreement with the theoretical values of 96.82 MeV and 96.40 MeV obtained with the Thomas-Fermi model [13] and listed in

AME2003 [12], respectively.

The observed ^{258}Rf half-life was $14.7^{+1.2}_{-1.0}$ ms, consistent with previously reported results [16, 19] and slightly longer than the 11±2 ms reported by Ghiorso *et al.* [20]. Based upon the 4 α-decay events and the 54 SF events observed at the two highest ^{26}Mg beam energies, and taking into account the differing efficiencies for detecting EVR-α-α and EVR-SF correlations, the α-decay branching ratio is 0.31±0.11, resulting in a partial half-life for α-decay of 47^{+24}_{-12} ms. This value is smaller than values calculated using our ^{258}Rf Q-value for α-decay and Hatsukawa *et al.* (146 ms) [18] or Parkhomenko *et al.* (210 ms) [17] α-decay systematics.

B. ^{259}Rf

Forty-five correlations (EVR-α, EVR-α-α) with properties in agreement with the known decay properties of ^{259}Rf and its daughters were observed at the beam energies of 133.0, 138.5, 144.5, and 151.4 MeV. From the measured rates of EVR- and α-like events, 5.4 random ^{259}Rf-like correlations were expected at those beam energies (see Table II). Twenty-seven of the forty-five correlations were observed under conditions where the expected number of random correlations was < 1. The ^{259}Rf half-life measured from these twenty-seven correlations is $2.5^{+0.4}_{-0.3}$ s, in agreement with the literature values of 3.1±1.3 s [21] and 3.4±1.7 s [19].

Three 8.4-MeV α-like events correlated to EVRs (see Table III) were observed during the pulsed portions of the 133.0 and 138.5 MeV irradiations. These correlations were assigned to the decay of ^{259}Lr, produced via an EC branch in ^{259}Rf. Since ^{259}Lr has a known SF branch of 0.25±0.03 [22], the observation of 'long-lived' EVR-SF

correlations is expected. Five SF events (see Table III) correlated in time (0.15 - 15 s) and position (±2.0 mm) to EVRs were observed at 133.0, 138.5 and 144.5 MeV. After correcting for differences in detection efficiencies of EVR-SF and EVR-α correlations, all five observed SF events can be accounted for by SF of the EC daughter, ^{259}Lr. The observation of 3 EVR-α, and 5 EVR-SF events is consistent with an ^{259}Rf EC branch of 0.15±0.04. Thus, previously reported SF branches in ^{259}Rf [19, 21, 23-25] are likely dominated by EC decay in ^{259}Rf followed by SF decay of ^{259}Lr. An EC branch in ^{259}Rf has not been observed when ^{259}Rf is produced as the decay product of ^{263}Sg [5, 14, 26-32], possibly indicating the presence of an isomer that is formed only in direct production of ^{259}Rf.

C. ^{260}Rf

Thirty-two short-lived (< 150 ms) EVR-SF correlations were observed at the three lowest ^{26}Mg beam energies. The assignment of these events to the 4*n* product, ^{260}Rf, is based upon the facts that i) both neighboring even-odd nuclides are significantly longer-lived, and ii) the highest reaction energy is only 5.7 MeV above the 6*n* exit channel threshold, making de-excitation by the 6*n* exit channel unlikely. The measured half-life for ^{260}Rf is $22.2^{+3.0}_{-2.4}$ ms, which is consistent with the previously reported half-life of 21±1 ms [19, 33]. The total kinetic energy (TKE) observed from the ^{260}Rf SF fragments was ~7 MeV above the TKE measured for ^{252}No under the same detection setup. Wild *et al*. [16] and Hulet *et al.* [33] have observed similar behavior for the SF of ^{260}Rf. The α-decay of ^{260}Rf followed by α-decay of ^{256}No was not observed, giving an α-decay branch upper limit of 0.35 at the 86% confidence level. The corresponding

partial α-decay half-life is > 64 ms. This compares well with the 0.20 upper limit for the α-decay branching ratio given by Lazarev *et al.* [34]. A predicted α-decay partial half-life of 1.4 s was calculated with the expected Q-value of 8.9 MeV [12] and using Hatsukawa α-decay systematics [18], corresponding to an expected α-branch of 0.016.

D. ^{261}Rf

^{261}Rf was produced in the ^{26}Mg(^{238}U, 3*n*)^{261}Rf reaction at the lowest excitation energy of 35.3 MeV. The direct production of ^{261}Rf from a 3*n* hot-fusion exit-channel has not been observed previously. Two isomers are known for ^{261}Rf. The first isomer, designated ^{261a}Rf, decays by either SF or α-particle emission (E_α = 8.51±0.05 MeV, I_α = 0.09, $t_{½} = 2.8^{+1.3}_{-0.7}$ s) [35]. The second isomer, designated ^{261b}Rf, has only been observed to decay by α-particle emission (E_α = 8.3 MeV, $t_{½}$ = 75±7 s), with an upper limit of 11% for decay by SF [36, 37].

We observed one correlated EVR-α-α decay chain with the following decay properties: ^{261}Rf (E_α = 8.34±0.05 MeV, τ = 103.2 s), ^{257}No (E_α = 8.30±0.05 MeV, τ = 12.2 s). This event was assigned to ^{261b}Rf and corresponds to a cross section of 28^{+92}_{-26} pb. A second event consisted of an EVR-SF decay chain with a SF energy of 173.3 MeV and a lifetime of 9.4 s. This event *could be* assigned to either isomer of ^{261}Rf. However, as discussed in the following section, there is only a 6% probability for observing a random EVR-SF correlation within 5 half-lives of ^{261a}Rf. If confirmed, this would represent the first observation of this isomer produced as an EVR. So far, ^{261a}Rf was only observed as the daughter of ^{265}Sg [1, 35, 38-40]. The addition of this second event would only increase the 3*n* cross section by 14%, to 32^{+93}_{-26} pb.

E. Random rates

Random rates for EVR-SF correlations were calculated by taking the observed number of SF events and multiplying by the probability of observing an EVR preceding the SF within the predefined time and position windows. The rate of EVR like events within a vertical position of ±2.0 mm was $0.4 – 8 \times 10^{-3}$ Hz, depending on beam energy. Over the course of the experiments, 128 events with energies above 100 MeV were observed in the focal plane detector. Of the 128 high energy events, 110 were assigned to the SF of the two short-lived isotopes ^{258}Rf and ^{260}Rf and one 14-μs EVR-SF correlation to the fission of an actinide fission isomer (most likely the 8-μs ^{239}Pu). All 128 SF-like events were used to calculate the random rates for the short-lived ^{258,260}Rf. As summarized in Table II, 0.02 random EVR-SF correlations are expect within 150 ms. Thus it is unlikely that any of the SF events assigned to ^{258}Rf or ^{260}Rf were of random origin. Of the 17 events that were not correlated to an EVR within 150 ms, five were correlated to EVRs within 15 s and were assigned to the SF decay of 6.1-s ^{259}Lr, produced through the EC of ^{259}Rf. These 17 SF events were used to calculate the EVR-SF random rates for the EC of ^{259}Rf. The expected number of random EVR-SF correlations within 15 s is 0.4. Thus it is very unlikely that more than one of the five observed EVR-SF correlations is of random origin.

EVR-α (EVR-α-α) random rates for ^{258,259}Rf were calculated by taking the observed number of EVRs and multiplying by the probability of observing one α (two α's) within the required time and position windows. For pulsed beam irradiations, decays of ^{259}Rf were identified through EVR-α correlations, while EVR-α-α correlations

were used during DC beam irradiations. The number of expected random ^{259}Rf-like correlations varied between 0.04 and 4.3, depending on beam conditions and energy (see Table II). Once the expected number of random correlations was taken into account, the cross sections observed during pulsed and DC beams were consistent. During the pulsed irradiations, 0.3 ^{259}Lr-like random EVR-α correlations are expected, resulting in a low probability of the 3 observed EVR-α being random. The expected number of random correlations for ^{258}Rf is 0.13, making it unlikely that any of the four observed EVR-α-α correlations are of random origin.

For ^{261}Rf there were 280 beam shut-offs, lasting 100 s each, that were initiated by the detection of a potential EVR-α correlation. A total of 8 α-particles in the energy range of 8.0 - 8.7 MeV were observed during the entire 2.8×10^4 s that the beam was shut off. With the requirement that correlated events occur within ±2.0 mm in the same strip as the potential EVR-α that initialized the beam shutoff, the expected number of randomly occurring EVR-α-α event sequences is 7×10^{-3} during the entire irradiation. In the search for ^{261}Rf EVR-SF correlations, the EVR-SF correlation time window was 350 s, 4.5 half-lives of the long-lived isomer, ^{261b}Rf. The expected number of random EVR-SF correlations within 350 s and ±2.0 mm is 1.7. However, the probability of observing a random EVR-SF correlation within 5 half-lives of ^{261a}Rf is only 6%.

IV. DISCUSSION

Excitation functions for the 4*n*, 5*n* and 6*n* exit channels for the ^{238}U(^{26}Mg, x*n*)$^{264-x}$Rf reaction are shown in Fig. 1. The data from pulsed beam irradiations were used to determine ^{259}Rf cross sections, due to the lower number of

expected random correlations. Horizontal error bars represent the range of compound nucleus excitation energies covered inside the target, while vertical error bars represent the uncertainties due to counting statistics [41]. The ^{238}U(^{26}Mg, 5*n*)^{259}Rf reaction has a maximum cross section of 1520±350 pb at a centroid beam energy of 139 MeV. The 6*n* exit channel, resulting in the production of ^{258}Rf, has the peak position at 146 MeV and a peak cross section that is 1.7 times smaller than that of the 5*n* exit channel. The maximum of the 4*n* exit channel is located at 128 MeV and the maximum cross section is ~4.8 times smaller than the maximum 5*n* cross section.

Historical precedence indicates that the 3*n* exit channel cross sections rapidly decrease with increasing $Z_{projectile}$ [42-44]. Recently, Dvorak *et al.* [35] have made the surprising observation of a 3*n* exit channel in the ^{248}Cm(^{26}Mg, 3*n*)^{271}Hs reaction, with a cross section that is comparable in magnitude to the 4*n* cross section. In this work, a dedicated irradiation searching for the 3*n* exit channel of the ^{26}Mg + ^{238}U reaction was performed. ^{261}Rf was observed to have a cross section of 28^{+92}_{-26} pb at a beam energy of 121.8 MeV, a factor of 10 times less than the peak of the 4*n* excitation function. These discoveries open the possibility of accessing long-lived neutron-rich nuclides of the transactinides utilizing hot fusion reactions with neutron-rich targets.

Figure 2 contains the systematics of Q-values for α-decay of even-even fermium (Fm), nobelium (No) and rutherfordium isotopes with N ~ 152. The plot contains accepted values for ^{256}Rf, fermium and nobelium isotopes [12] and a new value for ^{258}Rf (this work). In the absence of shell effects, a trend of smoothly decreasing Q-value with increasing N is expected. Deviation from the smooth trend is a direct measure of the variation of shell effect strength over the isotopic chain. The strength of the N = 152

deformed shell in rutherfordium appears to be similar to that in No and Fm.

Systematics of the partial SF half-lives of the even-even isotopes of fermium, nobelium, rutherfordium and seaborgium (Sg) are shown in Fig. 3. Partial SF half-lives for ^{260}Sg, ^{254}Rf, and the Fm and No isotopes were calculated using accepted values [12]. The plot also contains revised values for ^{258}Sg [45, 46], ^{262,264}Sg [5], ^{266}Sg [35] and ^{258,260}Rf (this work). SF half-lives of isotopic chains of even-Z elements with $96 \leq Z \leq 102$ are strongly peaked at N = 152, due to the influence of the deformed shells at N = 152 and Z = 100. Theoretical calculations by Smolańczuk *et al.* [47] demonstrated that small changes in the fission barrier, which are paralleled in the shell effects, should have a large effect on the fission half-lives. At N = 152, the shell effects are present, as observed in the α-decay Q-values, however the fission half-lives for rutherfordium and seaborgium remain constant across the N = 152 shell.

ACKNOWLEDGEMENTS

We gratefully acknowledge the operations staff of the 88-Inch Cyclotron for providing the intense beams of ^{26}Mg. Financial support was provided by the Office of High Energy and Nuclear Physics, Nuclear Physics Division of the U.S. Department of Energy, under contracts DE-AC02-05CH11231 and DE-AC03-76SF00098. R. Eichler acknowledges the financial support from the Swiss National Science Foundation (PA002-104962). J. Dvorak and A. Türler acknowledge financial support from the German Bundesministerium für Bildung und Forschung (BMBF Project No. 06MT194).

* Present address: Nuclear Science Division, Lawrence Berkeley National Laboratory,

Berkeley, CA 94720, USA

† Present address: National Superconducting Cyclotron Laboratory, Michigan State University, East Lansing, MI 48824, USA

‡ Present address: Department of Health Physics, University of Nevada, Las Vegas, Las Vegas, NV 89154, USA

[1] J. Dvorak, *et al.*, Phys. Rev. Lett. **97**, 242501 (2006).
[2] Y. T. Oganessian, J. Phys. G **34**, R165 (2007).
[3] S. Hofmann, *et al.*, Eur. Phys. J. A **32**, 251 (2007).
[4] R. Eichler, *et al.*, Nature **447**, 72 (2007).
[5] K. E. Gregorich, *et al.*, Phys. Rev. C **74**, 044611 (2006).
[6] K. E. Gregorich, *et al.*, Lawrence Berkeley National Laboratory Report; LBNL-63617 (2007).
[7] A. Türler, Habilitation Thesis, Universität Bern, Switzerland, 1999.
[8] W. Loveland, K. E. Gregorich, J. B. Patin, D. Peterson, C. Rouki, P. M. Zielinski, and K. Aleklett, Phys. Rev. C **66**, 044617 (2002).
[9] K. E. Gregorich, *et al.*, Phys. Rev. C **72**, 014605 (2005).
[10] K. E. Gregorich, *et al.*, Eur. Phys. J. A **18**, 633 (2003).
[11] J. F. Ziegler, Nucl. Instrum. Methods B **219-220**, 1027 (2004).
[12] G. Audi, O. Bersillon, J. Blachot, and A. H. Wapstra, Nucl. Phys. **A729**, 3 (2003).
[13] W. D. Myers and W. J. Swiatecki, Lawrence Berkeley National Laboratory Report; LBNL-36803 (1994); http://ie.lbl.gov/txt/ms.txt.
[14] C. M. Folden III, K. E. Gregorich, C. E. Düllmann, H. Mahmud, G. K. Pang, J. M. Schwantes, R. Sudowe, P. M. Zielinski, H. Nitsche, and D. C. Hoffman, Phys. Rev. Lett. **93**, 212702 (2004).
[15] *Table of Isotopes* 8th ed., edited by R. B. Firestone and V. S. Shirley (Wiley, New York, 1996).
[16] J. F. Wild, E. K. Hulet, R. W. Lougheed, K. J. Moody, B. B. Bandong, R. J. Dougan, and A. Veeck, J. Alloy. Comp. **213/214**, 86 (1994).
[17] A. Parkhomenko and A. Sobiczewski, Acta Phys. Pol. B **36**, 3095 (2005).
[18] Y. Hatsukawa, H. Nakahara, and D. C. Hoffman, Phys. Rev. C **42**, 674 (1990).
[19] L. P. Somerville, M. J. Nurmia, J. M. Nitschke, A. Ghiorso, E. K. Hulet, and R. W. Lougheed, Phys. Rev. C **31**, 1801 (1985).
[20] A. Ghiorso, M. Nurmia, J. Harris, K. Eskola, and P. Eskola, Phys. Rev. Lett. **22**, 1317 (1969).
[21] C. E. Bemis Jr., P. F. Dittner, R. L. Ferguson, D. C. Hensley, F. Plasil, and F. Pleasonton, Phys. Rev. C **23**, 555 (1981).
[22] T. M. Hamilton, *et al.*, Phys. Rev. C **46**, 1873 (1992).
[23] I. Zvára, V. Z. Belov, L. P. Chelnokov, V. P. Domanov, M. Hussonois, Y. S. Korotkin, V. A. Schegolev, and M. R. Shalayevsky, Inorganic and Nuclear

Chemistry Letters **7**, 1109 (1971).
[24] I. Zvara, Y. T. Chuburkov, V. Z. Belov, G. V. Buklanov, B. B. Zakhvataev, T. S. Zvarova, O. D. Maslov, R. Caletka, and M. R. Shalaevsky, Journal of Inorganic & Nuclear Chemistry **32**, 1885 (1970).
[25] I. Zvara, Y. T. Chuburkov, R. Tsaletka, and M. R. Shalaevskii, Soviet Radiochemistry **11**, 161 (1969).
[26] F. P. Heβberger (private communication).
[27] T. N. Ginter, *et al.*, Phys. Rev. C **67**, 064609 (2003).
[28] K. Morita, *et al.*, Eur. Phys. J. A **21**, 257 (2004).
[29] Y. A. Lazarev, *et al.*, Phys. Rev. Lett. **75**, 1903 (1995).
[30] Y. T. Oganessian, Nucl. Phys. **A583**, 823 (1995).
[31] K. E. Gregorich, M. R. Lane, M. F. Mohar, D. M. Lee, C. D. Kacher, E. R. Sylwester, and D. C. Hoffman, Phys. Rev. Lett. **72**, 1423 (1994).
[32] K. Nishio, *et al.*, Eur. Phys. J. A **29**, 281 (2006).
[33] E. K. Hulet, *et al.*, Phys. Rev. C **40**, 770 (1989).
[34] Y. A. Lazarev, *et al.*, Phys. Rev. C **62**, 064307 (2000).
[35] J. Dvorak, *et al.*, Phys. Rev. Lett. (submitted (2007)).
[36] B. Kadkhodayan, *et al.*, Radiochim. Acta **72**, 169 (1996).
[37] E. R. Sylwester, *et al.*, Radiochim. Acta **88**, 837 (2000).
[38] S. Hofmann, *et al.*, Eur. Phys. J. A **14**, 147 (2002).
[39] K. Morita, *et al.*, Journal of the Physical Society of Japan **76**, 043201 (2007).
[40] A. Türler, Eur. Phys. J. A **15**, 271 (2002).
[41] K. H. Schmidt, Eur. Phys. J. A **8**, 141 (2000).
[42] T. Sikkeland, J. Maly, and D. F. Lebeck, Phys. Rev. **169**, 1000 (1968).
[43] K. Eskola, P. Eskola, M. Nurmia, and A. Ghiorso, Phys. Rev. C **4**, 632 (1971).
[44] E. D. Donets, V. A. Shchegolev, and V. A. Ermakov, Sov. J. Nucl. Phys. **2**, 723 (1966).
[45] J. B. Patin, Lawrence Berkeley National Laboratory Report; LBNL-49593 (2002).
[46] F. P. Heβberger, *et al.*, Z. Phys. A **359**, 415 (1997).
[47] R. Smolańczuk, J. Skalski, and A. Sobiczewski, Phys. Rev. C **52**, 1871 (1995).
[48] R. Bass, Nucl. Phys. **A231**, 45 (1974).

Table I: Observed ^{258}Rf α-decay chains.

Beam Energy (MeV)	Excitation Energy (MeV)	Strip	E_{EVR} (MeV)	Vertical position (mm)	α-particle Energy (MeV)	Vertical position (mm)	Lifetime	Nuclide
144.5	55.8	31	5.56	-17.2±0.5	9.05±0.05	-18.0±0.3	46.09 ms	^{258}Rf
					8.09±0.05	-17.7±0.3	96.78 s	^{254}No
		3	7.62	-13.4±0.4	8.96±0.05	-13.2±0.3	6.24 ms	^{258}Rf
					8.08±0.05	-13.5±0.3	231.27 s	^{254}No
		16	5.39	24.6±0.5	9.05±0.05	24.4±0.3	9.70 ms	^{258}Rf
					8.10±0.05	24.0±0.3	43.63 s	^{254}No
151.4	62.0	34	5.89	-7.0±0.5	9.05±0.05	-6.8±0.3	11.14 ms	^{258}Rf
					8.05±0.05	-6.9±0.3	155.42 s	^{254}No

Table II: Cross sections, observed correlations and expected number of random correlations for the $^{238}U(^{26}Mg, xn)^{264-x}Rf$ reaction.

Beam Energy (MeV)	Excitation Energy (MeV)	ε_{BGS}	Beam Mode	Decay Mode	Expected Number of Random Correlations	Number of Observed Correlations	Cross Section (pb)
121.8	35.3	0.15	Pulsed	$^{260}Rf \xrightarrow{\alpha}$	0.9	0	50^{+30}_{-20}
				$^{260}Rf \xrightarrow{SF}$	0.003	11	
			DC	$^{260}Rf \xrightarrow{\alpha} {}^{256}No \xrightarrow{\alpha}$	0.6	0	40^{+80}_{-30}
				$^{260}Rf \xrightarrow{SF}$	0.001	2	
128.1	41.0	0.16	Pulsed	$^{260}Rf \xrightarrow{\alpha}$	0.1	0	170^{+80}_{-50}
				$^{260}Rf \xrightarrow{SF}$	0.003	9	
				$^{259}Rf \xrightarrow{\alpha}$	0.8	0	<120
				$^{259}Rf \xrightarrow{EC} {}^{259}Lr \xrightarrow{\alpha}$	0.1	0	

				$^{259}Rf \xrightarrow{EC} {}^{259}Lr \xrightarrow{SF}$ or $^{259}Rf \xrightarrow{SF}$	0	0	
133.0	45.4	0.18	Pulsed	$^{260}Rf \xrightarrow{\alpha}$	0.04	0	180^{+80}_{-60}
				$^{260}Rf \xrightarrow{SF}$	0.004	10	
				$^{259}Rf \xrightarrow{\alpha}$	0.4	4	440^{+300}_{-190}
				$^{259}Rf \xrightarrow{EC} {}^{259}Lr \xrightarrow{\alpha}$	0.1	1	
				$^{259}Rf \xrightarrow{EC} {}^{259}Lr \xrightarrow{SF}$ or $^{259}Rf \xrightarrow{SF}$	0.3	3	
138.5	50.4	0.19	Pulsed	$^{259}Rf \xrightarrow{\alpha}$	0.2	16	1560^{+460}_{-360}
				$^{259}Rf \xrightarrow{EC} {}^{259}Lr \xrightarrow{\alpha}$	0.1	2	
				$^{259}Rf \xrightarrow{EC} {}^{259}Lr \xrightarrow{SF}$ or $^{259}Rf \xrightarrow{SF}$	0	0	

				$^{258}\mathrm{Rf} \xrightarrow{\alpha} {}^{254}\mathrm{No} \xrightarrow{\alpha}$	0.05	0	110^{+90}_{-60}
				$^{258}\mathrm{Rf} \xrightarrow{\mathrm{SF}}$	0.005	8	
			DC	$^{259}\mathrm{Rf} \xrightarrow{\alpha} {}^{255}\mathrm{No} \xrightarrow{\alpha}$	4.3	20	1570^{+560}_{-430}
				$^{259}\mathrm{Rf} \xrightarrow{\mathrm{EC}} {}^{259}\mathrm{Lr} \xrightarrow{\mathrm{SF}}$ or $^{259}\mathrm{Rf} \xrightarrow{\mathrm{SF}}$	0.1	1	
				$^{258}\mathrm{Rf} \xrightarrow{\alpha} {}^{254}\mathrm{No} \xrightarrow{\alpha}$	0.08	0	310^{+160}_{-120}
				$^{258}\mathrm{Rf} \xrightarrow{\mathrm{SF}}$	0.001	14	
144.5	55.8	0.21	DC	$^{259}\mathrm{Rf} \xrightarrow{\alpha} {}^{255}\mathrm{No} \xrightarrow{\alpha}$	0.1	3	380^{+360}_{-200}
				$^{259}\mathrm{Rf} \xrightarrow{\mathrm{EC}} {}^{259}\mathrm{Lr} \xrightarrow{\mathrm{SF}}$ or $^{259}\mathrm{Rf} \xrightarrow{\mathrm{SF}}$	0.02	1	
				$^{258}\mathrm{Rf} \xrightarrow{\alpha} {}^{254}\mathrm{No} \xrightarrow{\alpha}$	0.002	3	770^{+200}_{-180}
				$^{258}\mathrm{Rf} \xrightarrow{\mathrm{SF}}$	0.003	34	

151.4	62.0	0.22	DC	$^{259}Rf \xrightarrow{\alpha} {}^{255}No \xrightarrow{\alpha}$	0.04	2	190^{+240}_{-120}
				$^{259}Rf \xrightarrow{EC} {}^{259}Lr \xrightarrow{SF}$	0.01	0	
				or $^{259}Rf \xrightarrow{SF}$			
				$^{258}Rf \xrightarrow{\alpha} {}^{254}No \xrightarrow{\alpha}$	0.0006	1	430^{+130}_{-110}
				$^{258}Rf \xrightarrow{SF}$	0.001	22	

Table III: Observed decay chains assigned to the electron capture of ^{259}Rf. SF energies are shown in boldface. For reconstructed SF events (events with energies in both the focal plane and upstream detectors), the energies detected in the focal plane and upstream detectors, respectively, are shown in parenthesis.

Beam Energy (MeV)	Beam Mode	Strip	E_{EVR} (MeV)	Vertical position (mm)	Energy (MeV)	Vertical position (mm)	Lifetime	Decay Mode
133.0	Pulsed	34	6.50	-20.9±0.5	8.46±0.05	-21.0±0.3	7.58 s	$^{259}Rf \xrightarrow{EC} {}^{259}Lr \xrightarrow{\alpha}$
		32	5.08	14.1±0.5	**180(113+67)**	14.5±1.5	3.74 s	$^{259}Rf \xrightarrow{EC} {}^{259}Lr \xrightarrow{SF}$ or $^{259}Rf \xrightarrow{SF}$
		14	6.19	15.4±0.5	**130**	15.5±1.5	14.63 s	$^{259}Rf \xrightarrow{EC} {}^{259}Lr \xrightarrow{SF}$ or $^{259}Rf \xrightarrow{SF}$
		27	6.04	1.7±0.5	**197(120+77)**	1.6±1.5	6.73 s	$^{259}Rf \xrightarrow{EC} {}^{259}Lr \xrightarrow{SF}$ or $^{259}Rf \xrightarrow{SF}$

138.5	Pulsed	26	9.17	-26.8±0.4	8.42±0.05	-26.5±0.3	3.89 s	$^{259}Rf \xrightarrow{EC} {}^{259}Lr \xrightarrow{\alpha}$
		30	6.95	23.5±0.5	8.44±0.05	23.4±0.3	0.90 s	$^{259}Rf \xrightarrow{EC} {}^{259}Lr \xrightarrow{\alpha}$
	DC	11	7.02	-8.1±0.4	**203**	-7.8±1.5	9.77 s	$^{259}Rf \xrightarrow{EC} {}^{259}Lr \xrightarrow{SF}$ or $^{259}Rf \xrightarrow{SF}$
144.5	DC	13	7.21	27.4±0.4	**110**	27.2±1.5	2.97 s	$^{259}Rf \xrightarrow{EC} {}^{259}Lr \xrightarrow{SF}$ or $^{259}Rf \xrightarrow{SF}$

FIG 1: (color online) Cross section for the 3*n* exit channel and excitation functions for the 4*n*, 5*n*, and 6*n* exit channels of the $^{238}U(^{26}Mg, xn)^{264-x}Rf$ reaction. The arrow at 134.6 MeV represents the position of the Bass barrier [48]. Lines are a Gaussian smoothly joined to an exponential on the high energy side fitted to the experimental data according to the procedure described in [6].

FIG 2: (color online) Q-values for the α-decay of the even-even isotopes of Fm, No and Rf. Error bars are smaller than the size of the symbols.

FIG 3: (color online) Partial spontaneous fission half-lives for even-even isotopes of Fm, No, Rf and Sg. Error bars are smaller than the size of the symbols.

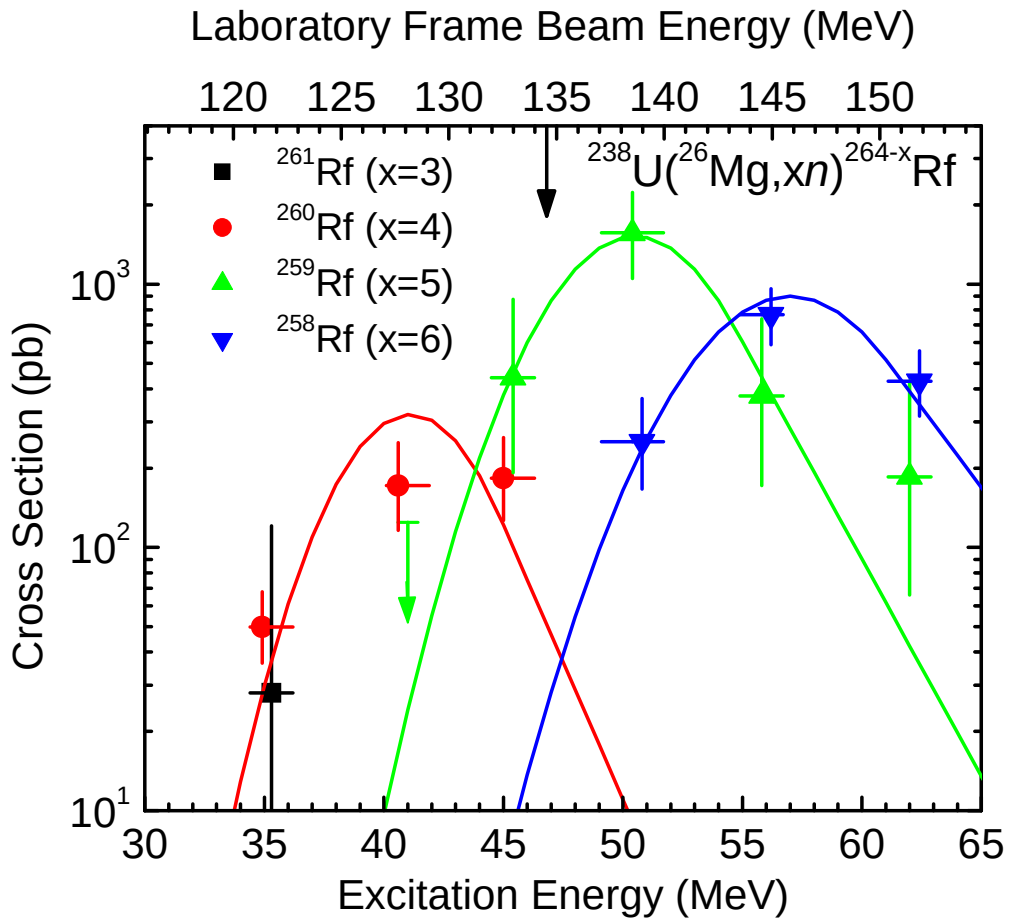
Laboratory Frame Beam Energy (MeV)
120 125 130 135 140 145 150
^{261}Rf (x=3)
^{260}Rf (x=4)
^{259}Rf (x=5)
^{258}Rf (x=6)
^{238}U(^{26}Mg,xn)$^{264-x}$Rf
Cross Section (pb)
10^3
10^2
10^1
30 35 40 45 50 55 60 65
Excitation Energy (MeV)

FIG 1

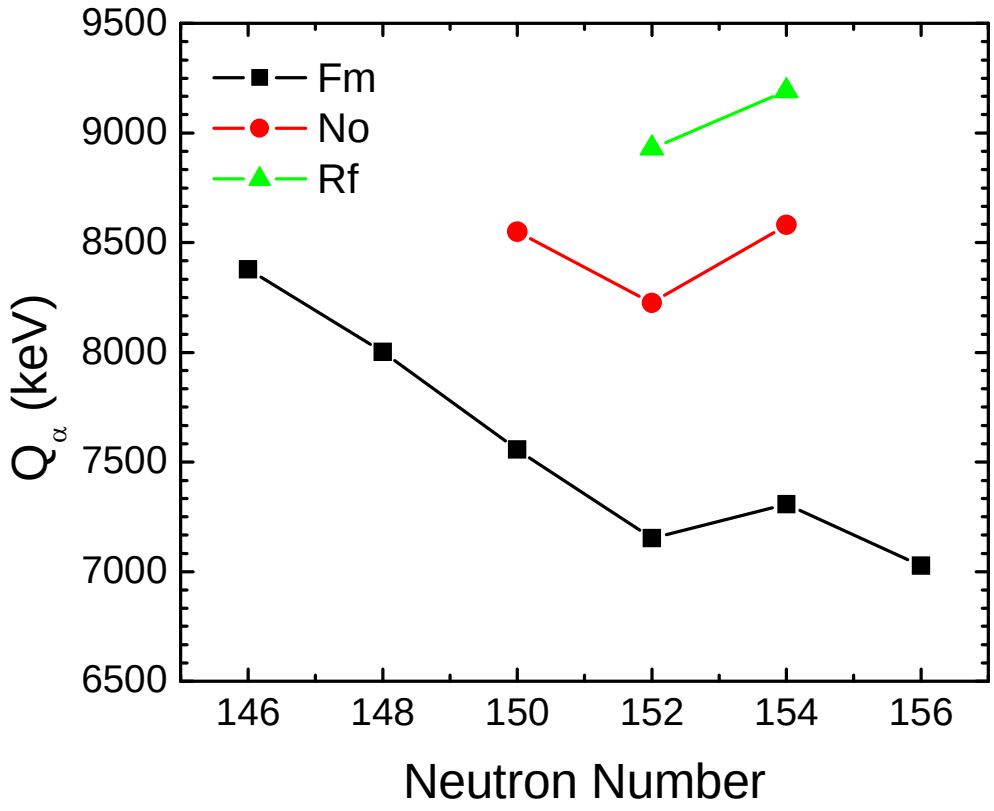
9500
9000
8500
8000
7500
7000
6500
Q$_\alpha$ (keV)
Fm
No
Rf
146
148
150
152
154
156
Neutron Number

FIG 2

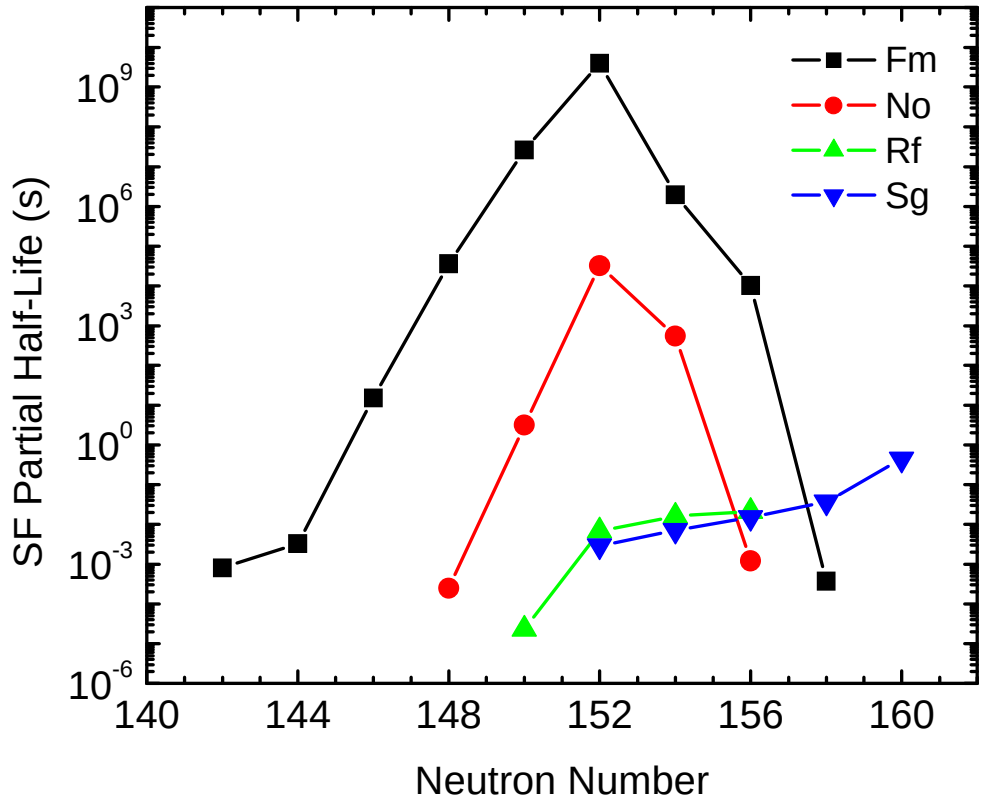
SF Partial Half-Life (s)
10^{9}
10^{6}
10^{3}
10^{0}
10^{-3}
10^{-6}
140
144
148
152
156
160
Neutron Number
Fm
No
Rf
Sg

FIG 3